R & M No.3815

R &M No.3815

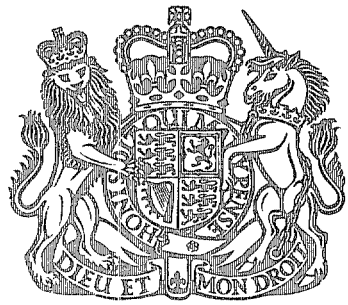

PROCUREMENT EXECUTIVE, MINISTRY OF DEFENCE

Aeronautical Research Council
Reports and Memoranda

SIMPLIFIED THREE-DIMENSIONAL ANALYSIS AND DESIGN OF FIBRE REINFORCED ANNULAR DISCS SURROUNDING A CIRCULAR HOLE IN A FLAT PLATE UNDER VARIOUS LOADING CONDITIONS

by

E.H. Mansfield, FRS
Structures Dept., RAE Farnborough

London: Her Majesty's Stationery Office
1978

PRICE £4 NET

SIMPLIFIED THREE-DIMENSIONAL ANALYSIS AND DESIGN OF FIBRE REINFORCED ANNULAR DISCS SURROUNDING A CIRCULAR HOLE IN A FLAT PLATE UNDER VARIOUS LOADING CONDITIONS

by E.H. Mansfield, FRS

Structures Department, RAE Farnborough

REPORTS AND MEMORANDA No.3815*

November 1976

SUMMARY

A flat plate containing a circular hole is subjected to arbitrary bi-axial stresses at infinity; adajcent to the hole and bonded symmetrically to both sides of the plate are cylindrically wound fibre composite annular discs. The relatively low shear moduli of the composite cause shear lag effects normal to the plane of the plate. The present paper shows that it is possible to allow for these effects, within the framework of a two-dimensional analysis, by the use of an *effective* thickness for the reinforcement which is a function of the overall geometry, the elastic moduli and the type of loading. The practically important case of applied uniaxial stress is considered in detail and it is shown how, for a given weight of reinforcement, the reinforcement cross-section can be chosen to minimise the peak stresses.

---

* Replaces RAE Technical Report 76148 - ARC 37224

LIST OF CONTENTS

1 INTRODUCTION

In many structures, particularly those in the aerospace field, the saving of weight is of paramount importance. Aircraft structures, for example, are generally of stressed skin construction in which loads are carried primarily by membrane stresses in flat or curved plates. When such a plate contains a hole there is a redistribution of stress in the vicinity of the hole and a consequent weakening of the plate. To counteract this the designer reinforces the plate and a considerable body of research literature is devoted to this problem. There are, needless to say, conflicting requirements. Thus, confining attention to the flat plate, the optimum reinforcement is symmetrically disposed about the mid-plane so as to avoid the introduction of bending stresses, but this is not practicable if the plate forms part of the aerodynamic surface; similarly, according to classical two-dimensional theory the optimum reinforcement generally consists of a compact member following the (curved) boundary of the hole and carrying direct rather than bending loads, but this compactness can lead to difficulties in transferring the load from the plate and, indeed, in transferring load to those parts of the reinforcement furthermost from the plane of the plate.

There is now renewed interest in this problem because of the introduction of fibre composites, particularly those based on carbon (CFRP). Such composites show up to maximum advantage when they carry purely tensile or compressive loads for these require a unidirectional array of fibres. In these applications the potential gains are considerable because the specific strength of unidirectional CFRP, for example, is some four to five times that of aluminium alloys.

Here we consider an infinite isotropic elastic plate containing a circular hole whose boundary is reinforced with cylindrically wound fibre composite annular discs symmetrically disposed about the mid-plane of the plate. Such a reinforcement primarily carries hoop loads, although the transfer of load from the plate necessarily introduces shearing forces N_{rz}, $N_{\theta z}$ (z normal to the plane of the plate) and therefore brings into play the relatively poor transverse properties of the composite. Strictly speaking the reinforcement should therefore be analysed in a three-dimensional manner but, because of the complexities involved, this has been possible[1] only for the rotationally symmetric case of a remotely applied uniform radial tension - and then only with the simplifying assumption of an infinite modulus E_z. This analysis shows that the 'shear lag' effects normal to the plane of the plate reduce the effectiveness of those parts of the reinforcement furthermost from the plate,

and the effect is significant for reinforcements with compact cross-sections; for shallow plate-like reinforcements a two-dimensional analysis, which embodies the additional assumption of an infinite shear modulus G_{rz}, is adequate. Such a two-dimensional analysis is given by McKenzie and Webber[2] for remotely applied radial tension and shear, thus yielding by superposition the practically important case of uniaxial tension.

The present paper presents approximate three-dimensional solutions for these same loading conditions. Account is taken of the shear lag effects normal to the plane of the plate by the introduction of appropriate efficiency factors for the reinforcement; these factors determine an effective thickness of the reinforcement which is used in a subsequent two-dimensional analysis. When E_z is assumed infinite the method yields excellent agreement with the results of the three-dimensional analysis of Ref.1; indeed, the method is expected to yield even more realistic results because it is further refined to take account of the finite value of E_z.

2 NOTATION (see also Fig.1)

a_{ij}	3 × 3 matrix defined by equation (4-5)
E, G	Young's modulus, shear modulus
h	thickness of annular reinforcing disc
N	force per unit length
r, θ	polar coordinates
r_1, r_2	radius of hole, outer radius of annular discs
r*	$\frac{1}{2}(r_1 + r_2)$
t	thickness of plate
u, v	radial and tangential displacement
V	volume of reinforcement, see equations (7-1) to (7-3)
w	width of reinforcing annulus, $r_2 - r_1$
z	normal distance from surface of plate
α_{ij}, β_{ij}	3 × 3 matrices defined by equations (4-1) and (4-2)
γ, ε	shear strain, direct strain
ξ	z/h
η	efficiency factor
κ, ω	parameters defined by equation (4-12)
λ_i	parameters defined by equations (5-5), (5-26) and (5-27)

μ	r_2/r_1
ν	Poisson's ratio
ρ	r/r_1
σ, τ	direct stress, shear stress
ϕ	parameter defined by equation (5-14)
Φ	stress function
ψ	parameter defined by equation (6-1)

Suffices

P, R	refer to plate and reinforcement, respectively
T, S	refer to uniform radial tension and shear, respectively.

3 THE STRUCTURE AND MATERIAL PROPERTIES

A flat plate of thickness t contains a circular hole of radius r_1 and is reinforced over an annulus from r_1 to r_2 by cylindrically wound fibre composite annular discs of thickness h symmetrically disposed about the centre line of the plate, as shown in Fig.1. The plate is isotropic with Young's modulus E and Poisson's ratio ν. The fibre reinforced discs possess cylindrical orthotropy with Young's moduli E_θ, E_r, E_z, shear moduli $G_{r\theta}$, G_{rz}, $G_{\theta z}$ and Poisson's ratios $\nu_{\theta r}$, $\nu_{r\theta}$, etc.

Generalised plane stress conditions are assumed throughout for the plate, while in section 4 the fibre reinforced discs are represented by discs of effective thickness ηh under generalised plane stress, thus confining attention to the moduli E_θ, E_r, $G_{r\theta}$. Account is taken of the moduli E_z, G_{rz}, $G_{\theta z}$ in section 5 which determines the 'reinforcement efficiency factor' η.

Finally we note that if the fibres are disposed isotropically or in a random manner over the reinforcement cross-section we have

$$\left.\begin{aligned} E_r &= E_z \quad , \\ \text{and} \qquad G_{r\theta} &= G_{\theta z} \quad . \end{aligned}\right\} \tag{3-1}$$

4 GENERAL TWO-DIMENSIONAL FORMULATION

Apart from the introduction of the factor η the analysis in this section is based entirely on earlier work by McKenzie and Webber[2], Lekhnitskii[3] and Mansfield[4].

4.1 Stress-strain relations

In the plate P the stress-strain relations are given by

$$\left.\begin{aligned} \{\varepsilon_r, \varepsilon_\theta, \gamma_{r\theta}\} &= [\alpha_{ij}]\{\sigma_r, \sigma_\theta, \tau_{r\theta}\}_P \quad , \\ \text{where } [\alpha_{ij}] &\text{ is a symmetrical } 3 \times 3 \text{ matrix in which} \\ \alpha_{11} = \alpha_{22} &= 1/E \quad , \quad \alpha_{12} = \alpha_{21} = -\nu/E \quad , \\ \alpha_{33} = 2(1+\nu)/E &\quad , \quad \alpha_{13} = \alpha_{23} = \alpha_{31} = \alpha_{32} = 0 \quad , \end{aligned}\right\} \tag{4-1}$$

and E is Young's modulus and ν is Poisson's ratio.

Similarly, in the material of the reinforcing annulus R

$$\left.\begin{aligned} \{\varepsilon_r, \varepsilon_\theta, \gamma_{r\theta}\} &= [\beta_{ij}]\{\sigma_r, \sigma_\theta, \tau_{r\theta}\}_R \quad , \\ \text{where} \quad \beta_{11} = 1/E_r \quad , &\quad \beta_{22} = 1/E_\theta \quad , \quad \beta_{12} = \beta_{21} = -\nu_{\theta r}/E_\theta \quad , \\ \beta_{33} = 1/G_{r\theta} \quad , &\quad \beta_{13} = \beta_{23} = \beta_{31} = \beta_{32} = 0 \quad . \end{aligned}\right\} \tag{4-2}$$

These equations may be inverted to give

$$\left.\begin{aligned} \{\sigma_r, \sigma_\theta, \tau_{r\theta}\}_P &= [\alpha_{ij}]^{-1}\{\varepsilon_r, \varepsilon_\theta, \gamma_{r\theta}\} \quad , \\ \{\sigma_r, \sigma_\theta, \tau_{r\theta}\}_R &= [\beta_{ij}]^{-1}\{\varepsilon_r, \varepsilon_\theta, \gamma_{r\theta}\} \quad . \end{aligned}\right\} \tag{4-3}$$

Now in the range $r_1 < r < r_2$ the stress resultants are given by

$$\{N_r, N_\theta, N_{r\theta}\} = t\{\sigma_r, \sigma_\theta, \tau_{r\theta}\}_P + 2\eta h\{\sigma_r, \sigma_\theta, \tau_{r\theta}\}_R \tag{4-4}$$

where η is an efficiency factor which takes account of the shear lag effects normal to the plane of the plate. Hence from equations (4-3) and (4-4) we obtain

$$\left.\begin{aligned} \{\varepsilon_r,\ \varepsilon_\theta,\ \gamma_{r\theta}\} &= [a_{ij}]\{N_r,\ N_\theta,\ N_{r\theta}\} \\ \text{where} \qquad [a_{ij}] &= \left[t[\alpha_{ij}]^{-1} + 2\eta h[\beta_{ij}]^{-1}\right]^{-1} \quad . \end{aligned}\right\} \tag{4-5}$$

Finally, we relate the stresses to the stress resultants by means of equations (4-1), (4-2) and (4-5):

$$\left.\begin{aligned} \{\sigma_r,\ \sigma_\theta,\ \tau_{r\theta}\}_P &= [\alpha_{ij}]^{-1}[a_{ij}]\{N_r,\ N_\theta,\ N_{r\theta}\} \\ \{\sigma_r,\ \sigma_\theta,\ \tau_{r\theta}\}_R &= [\beta_{ij}]^{-1}[a_{ij}]\{N_r,\ N_\theta,\ N_{r\theta}\} \end{aligned}\right\} \tag{4-6}$$

valid in the range $r_1 < r < r_2$, while for $r > r_2$

$$\{\sigma_r,\ \sigma_\theta,\ \tau_{r\theta}\}_P = \{N_r,\ N_\theta,\ N_{r\theta}\}/t \quad . \tag{4-7}$$

4.2 Equilibrium and compatibility

The stress resultants satisfy the following equations of equilibrium

$$\left.\begin{aligned} \frac{\partial N_r}{\partial r} + \frac{N_r - N_\theta}{r} + \frac{1}{r}\frac{\partial N_{r\theta}}{\partial \theta} &= 0 \quad , \\ \frac{1}{r}\frac{\partial N_\theta}{\partial \theta} + \frac{\partial N_{r\theta}}{\partial r} + \frac{2N_{r\theta}}{r} &= 0 \quad , \end{aligned}\right\} \tag{4-8}$$

which are satisfied by the introduction of a stress function Φ such that

$$\left.\begin{aligned} N_r &= \frac{1}{r}\frac{\partial \Phi}{\partial r} + \frac{1}{r^2}\frac{\partial^2 \Phi}{\partial \theta^2} \quad , \\ N_\theta &= \frac{\partial^2 \Phi}{\partial r^2} \quad , \\ N_{r\theta} &= \frac{1}{r^2}\frac{\partial \Phi}{\partial \theta} - \frac{1}{r}\frac{\partial^2 \Phi}{\partial r \partial \theta} \quad . \end{aligned}\right\} \tag{4-9}$$

Now in terms of the displacements u, v the strains are given by

$$\left.\begin{aligned} \varepsilon_r &= \frac{\partial u}{\partial r} \quad , \\ \varepsilon_\theta &= \frac{u}{r} + \frac{1}{r}\frac{\partial v}{\partial \theta} \quad , \\ \gamma_{r\theta} &= \frac{1}{r}\frac{\partial u}{\partial \theta} + r\frac{\partial}{\partial r}\left(\frac{v}{r}\right) \quad , \end{aligned}\right\} \tag{4-10}$$

from which the displacements can be eliminated to yield the equation of compatibility:

$$\frac{\partial^2 \varepsilon_r}{\partial \theta^2} - r\frac{\partial \varepsilon_r}{\partial r} + \frac{\partial}{\partial r}\left\{r^2\left(\frac{\partial \varepsilon_\theta}{\partial r} - \frac{1}{r}\frac{\partial \gamma_{r\theta}}{\partial \theta}\right)\right\} = 0 \quad . \tag{4-11}$$

Equations (4-1), (4-5), (4-7) and (4-9) enable us to express equation (4-11) in terms of the stress function Φ, whence

$$\left.\begin{aligned} &\left[\kappa\Delta_r^4 + 2\omega\Delta_r^2\Delta_\theta + \Delta_\theta^2 - (1 + \kappa + 2\omega)\Delta_r^2\right]\Phi = 0 \quad , \\ &\text{where in the range } r_1 < r < r_2 : \\ &\kappa = a_{22}/a_{11} \quad , \quad \omega = (a_{12} + \tfrac{1}{2}a_{33})/a_{11} \quad , \\ &\text{and for } r > r_2 : \\ &\kappa = \omega = 1 \quad , \end{aligned}\right\} \tag{4-12}$$

and the differential operators Δ_r, Δ_θ are defined by

$$\left.\begin{aligned} \Delta_r F &= r^2\frac{\partial}{\partial r}\left(\frac{F}{r}\right) \quad , \\ \Delta_\theta F &= \left(1 + \frac{\partial^2}{\partial \theta^2}\right)F \quad . \end{aligned}\right\} \tag{4-13}$$

5 THE EFFICIENCY FACTORS η

In this section we derive expressions for the efficiency factors η_T, η_S appropriate to a uniformly applied radial tension or shear respectively. Shear lag effects normal to the plane of the plate stem from the finite and relatively low values of the shear moduli G_{rz}, $G_{\theta z}$ in comparison with E_θ. The moduli E_r, $G_{r\theta}$ which are also small in comparison with E_θ play a negligible role in these shear lag effects and they are then assumed to be zero. Account is taken of the actual values of E_r, $G_{r\theta}$ in the subsequent two-dimensional analyses which assume an effective thickness $\eta_T h$ or $\eta_S h$ for the annular reinforcement. It is first assumed that the displacement normal to the plane of the plate is zero, which is equivalent to an assumption of infinite E_z, but this assumption is later relaxed.

In terms of the displacements u, v the stress-strain relations in an element of the reinforcement are now given by

$$\left.\begin{aligned} \sigma_\theta &= E_\theta \left(\frac{u}{r} + \frac{1}{r}\frac{\partial v}{\partial \theta}\right) \quad , \\ \tau_{rz} &= G_{rz}\frac{\partial u}{\partial z} \quad , \\ \text{and} \qquad \tau_{\theta z} &= G_{\theta z}\frac{\partial v}{\partial z} \quad . \end{aligned}\right\} \tag{5-1}$$

The equations of equilibrium in the radial and circumferential directions are

$$\left.\begin{aligned} \frac{\partial \tau_{rz}}{\partial z} - \frac{1}{r}\sigma_\theta &= 0 \quad , \\ \text{and} \qquad \frac{\partial \tau_{\theta z}}{\partial z} + \frac{1}{r}\frac{\partial \sigma_\theta}{\partial \theta} &= 0 \quad . \end{aligned}\right\} \tag{5-2}$$

5.1 η_T for applied radial tension

In the case of a uniformly applied radial tension the displacement v is zero and substitution of equations (5-1) into equations (5-2) yields

$$\frac{\partial^2 u}{\partial z^2} - \left(\frac{E_\theta}{G_{rz}}\right)\frac{u}{r^2} = 0 \quad . \tag{5-3}$$

Now the shear lag effect is of significance only for compact reinforcements in which $(r_2 - r_1)$ is small in comparison with r_1 . It is thus adequate, bearing in mind the approximations already introduced, to treat r as constant in equation (5-3) and equal to the average value $\frac{1}{2}(r_1 + r_2)$ represented by r^* . Equation (5-3) may now be integrated to give the following z-wise variation of u :

$$u = f_1(r)e^{\lambda_1 \xi} + f_2(r)e^{-\lambda_1 \xi} \quad , \tag{5-4}$$

where

$$\left.\begin{aligned} \xi &= z/h \quad , \\ \lambda_1 &= \frac{h}{r^*}\left(\frac{E_\theta}{G_{rz}}\right)^{\frac{1}{2}} \quad . \end{aligned}\right\} \tag{5-5}$$

The boundary conditions are that τ_{rz} is zero at $z = h$, whence

$$u = \frac{\cosh \lambda_1(1 - \xi)}{\cosh \lambda_1}[u]_{z=0} \quad , \tag{5-6}$$

and similarly

$$\sigma_\theta = \frac{\cosh \lambda_1(1 - \xi)}{\cosh \lambda_1}[\sigma_\theta]_{z=0} \quad . \tag{5-7}$$

Integration of σ_θ over the range $0 \leqslant z \leqslant h$ now yields the following expression for the efficiency factor η_T ,

$$\eta_T = \frac{\int_0^h \sigma_\theta dz}{h[\sigma_\theta]_{z=0}}$$

$$= \frac{1}{\lambda_1}\tanh \lambda_1 \quad . \tag{5-8}$$

In the next section we modify this expression to take approximate account of the finite value of E_z . The good agreement already found between a two-dimensional analysis based on equation (5-8) and Ref.1, which is a rigorous

three-dimensional analysis but with the assumption of an infinite value of E_z, is adequate justification for attempting this further improvement.

5.1.1 Effect of finite modulus E_z

The assumption of an infinite value for E_z necessarily results in an overestimate of the value of η_T although this is significant only when the reinforcing annulus has a compact cross-section. In such circumstances an approximate allowance can be made for the finite value of E_z by treating the reinforcing annulus as a (very) short cylinder. Thus within the framework of elementary shell theory[5], modified to take account of shear deformation, we can write

$$D_z \frac{d^4 u_b}{dz^4} + E_\theta \frac{wu}{r^{*2}} = 0 \quad , \tag{5-9}$$

where u_b is the component of radial displacement due to bending, w is the width of reinforcement $(r_2 - r_1)$ and D_z is the flexural rigidity of the 'shell', given adequately by

$$D_z = \frac{1}{12} E_z w^3 \quad . \tag{5-10}$$

Similarly, the deflexion due to shear u_s satisfies the equation

$$G_{rz} w \frac{d^2 u_s}{dz^2} - E_\theta \frac{wu}{r^{*2}} = 0 \quad . \tag{5-11}$$

Now

$$u = u_b + u_s \quad , \tag{5-12}$$

and hence equations (5-9) to (5-11) yield

$$\frac{d^4 u}{d\xi^4} - \lambda_1^2 \frac{d^2 u}{d\xi^2} + 4\phi^2 u = 0 \quad , \tag{5-13}$$

where ξ, λ_1 are as previously defined and

$$\phi = \frac{h^2}{wr^*} \left(\frac{3E_\theta}{E_z} \right)^{\frac{1}{2}} \quad . \tag{5-14}$$

The general solution of equation (5-13) can be expressed in the form

$$u = \sum_{i=1}^{4} B_i p_i^4 e^{p_i \xi} \tag{5-15}$$

where the p_i are the roots of the equation

$$p_i^4 - \lambda_1^2 p_i^2 + 4\phi^2 = 0 \quad . \tag{5-16}$$

Substitution of equation (5-15) into equations (5-9) and (5-11) and integration yields

$$\left.\begin{aligned} u_b &= -4\phi^2 \sum_i B_i e^{p_i \xi} \quad , \\ u_s &= \lambda_1^2 \sum_i B_i p_i^2 e^{p_i \xi} \quad . \end{aligned}\right\} \tag{5-17}$$

The boundary conditions are that

$$\left.\begin{aligned} u = u_0 \quad , \quad \frac{du_b}{d\xi} = 0 \quad , \\ \text{at} \quad \xi = 0 \quad , \end{aligned}\right\} \tag{5-18}$$

and

$$\left.\begin{aligned} \frac{d^2 u_b}{d\xi^2} = \frac{d^3 u_b}{d\xi^3} = \frac{du_s}{d\xi} = 0 \quad , \\ \text{at} \quad \xi = 1 \quad , \end{aligned}\right\} \tag{5-19}$$

hence

$$\left.\begin{aligned} \sum_i B_i p_i^4 &= u_0 \quad , \\ \sum_i B_i p_i = \sum_i B_i p_i^2 e^{p_i} &= \sum_i B_i p_i^3 e^{p_i} = 0 \quad . \end{aligned}\right\} \tag{5-20}$$

In terms of the coefficients B_i the efficiency factor is given by

$$\left.\begin{aligned} \eta_T &= \frac{1}{u_0}\int_0^1 u\,d\xi \\ &= \frac{1}{u_0}\sum_i B_i p_i^3 (e^{p_i} - 1) \quad . \end{aligned}\right\} \tag{5-21}$$

The resulting analytical expression for η_T is very cumbersome, particularly when the p_i are complex. To simplify matters we have determined η_T numerically over the practical range of values of λ_1, ϕ and find that there is excellent agreement with the following empirical expression which was chosen because it gives the correct variation with λ_1 when ϕ is zero, the correct variation for small values of λ_1, ϕ and the correct asymptotic variation with ϕ when λ_1 is zero:

$$\left.\begin{aligned} \eta_T &\approx \frac{1}{\lambda_1^*}\tanh \lambda_1^* \quad , \\ \text{where} \qquad \lambda_1^* &= \left[\lambda_1^2 + \phi \tanh\left(\frac{3}{5}\phi\right)\right]^{\frac{1}{2}} \quad . \end{aligned}\right\} \tag{5-22}$$

5.2 η_S for applied shear

The analysis for an applied shear, with E_z assumed infinite, is only slightly more complex than that for uniform radial tension despite the fact that account must now be taken of the tangential displacement. Thus substitution of equations (5-1) into equation (5-2) yields

$$\left.\begin{aligned} G_{rz}\frac{\partial^2 u}{\partial z^2} - \frac{E_\theta}{r^2}\left(u + \frac{\partial v}{\partial \theta}\right) &= 0 \quad , \\ G_{\theta z}\frac{\partial^2 v}{\partial z^2} + \frac{E_\theta}{r^2}\left(\frac{\partial u}{\partial \theta} + \frac{\partial^2 v}{\partial \theta^2}\right) &= 0 \quad . \end{aligned}\right\} \tag{5-23}$$

Now it can be shown from this simplified analysis or, indeed, from a rigorous three-dimensional approach that the θ-variation of u, v is such that

$$\left.\begin{aligned} u &= \bar{u}\cos 2\theta \\ v &= \bar{v}\sin 2\theta \quad , \end{aligned}\right\} \tag{5-24}$$

where $\bar{u}$, $\bar{v}$ are independent of θ. Substitution of equation (5-24) into equation (5-23) and division throughout by $\cos 2\theta$, $\sin 2\theta$ respectively gives

$$\left.\begin{aligned} \frac{\partial^2 \bar{u}}{\partial \xi^2} - \lambda_1^2(\bar{u} + 2\bar{v}) &= 0 \quad , \\ \frac{\partial^2 \bar{v}}{\partial \xi^2} - 2\lambda_2^2(\bar{u} + 2\bar{v}) &= 0 \quad , \end{aligned}\right\} \tag{5-25}$$

where ξ, λ_1 are as defined in equation (5-5) and

$$\lambda_2 = \frac{h}{r^*}\left(\frac{E_\theta}{G_{\theta z}}\right)^{\frac{1}{2}} \quad . \tag{5-26}$$

Equation (5-25) may be integrated to give

$$\left.\begin{aligned} \bar{u} + 2\bar{v} &= f_1 e^{\lambda_3 \xi} + f_2 e^{-\lambda_3 \xi} \\ &= U \quad , \quad \text{say,} \\ \text{where} \qquad \lambda_3 &= (\lambda_1^2 + 4\lambda_2^2)^{\frac{1}{2}} \quad , \end{aligned}\right\} \tag{5-27}$$

and

$$\left.\begin{aligned} \bar{u} &= \frac{\lambda_1^2}{\lambda_3^2} U + 2k_1 + 2k_2 \xi \\ \bar{v} &= \frac{2\lambda_2^2}{\lambda_3^2} U - k_1 - k_2 \xi \quad . \end{aligned}\right\} \tag{5-28}$$

The boundary conditions are such that τ_{rz}, $\tau_{\theta z}$ vanish at $z = h$, whence

$$\left.\begin{aligned} k_2 &= 0 \\ U &= \frac{\cosh \lambda_3(1-\xi)}{\cosh \lambda_3}[U]_{z=0} \quad , \\ \text{and} \\ \sigma_\theta &= \frac{\cosh \lambda_3(1-\xi)}{\cosh \lambda_3}[\sigma_\theta]_{z=0} \quad . \end{aligned}\right\} \qquad (5\text{-}29)$$

(The terms involving k_1 correspond to deformations in which ε_θ vanishes.)

Corresponding to equation (5-8) we now find

$$\eta_S = \frac{1}{\lambda_3}\tanh \lambda_3 \quad . \qquad (5\text{-}30)$$

5.2.1 Effect of finite modulus E_z

For the case of uniform radial tension the finite value of E_z caused a reduction in the value of η due primarily to a bending of the (compact) reinforcement cross-section. As such it resulted in an increase in the value of λ_1, i.e. an effective reduction in the modulus G_{rz}.

The same effective reduction in the modulus G_{rz} occurs in the present instance but there is no comparable effect in the transfer of shears $N_{r\theta}$. This is because the 'half wavelength' of the shears $N_{r\theta}$, namely $\frac{\pi}{2}r$, is much greater than h. Accordingly we take account of the finite value of E_z in the case of applied shear by writing

$$\left.\begin{aligned} \eta_S &\approx \frac{1}{\lambda_3^*}\tanh \lambda_3^* \quad , \\ \text{where} \quad \lambda_3^* &= (\lambda_1^{*2} + 4\lambda_2^2)^{\frac{1}{2}} \quad . \end{aligned}\right\} \qquad (5\text{-}31)$$

Note that $\lambda_3^* > \lambda_1^*$ and hence $\eta_S < \eta_T$ and the z-wise shear lag effects are thus more significant for shear loading than for uniform radial tension.

5.3 Higher harmonic loadings

In the problems discussed here θ-variations other than $\begin{pmatrix}\sin\\ \cos\end{pmatrix} 2\theta$ do not occur, but for more complex loadings or boundary conditions they will occur. In such circumstances we note that if

$$\left.\begin{aligned} u &= \bar{u} \cos m\theta \quad , \\ v &= \bar{v} \sin m\theta \quad , \end{aligned}\right\} \tag{5-32}$$

an analysis similar to that previously given, with E_z infinite, shows that

$$\left.\begin{aligned} \eta_m \text{ , say } &= \frac{1}{\lambda} \tanh \lambda \quad , \\ \text{where} \qquad \lambda &= (\lambda_1^2 + m^2\lambda_2^2)^{\frac{1}{2}} \quad . \end{aligned}\right\} \tag{5-33}$$

Finally we emphasise again that the concept of a single efficiency factor for the reinforcement is valid only within the context of a given harmonic load distribution. The case of an applied uniaxial tension, for example, requires separate analyses for its component harmonic parts, namely uniform radial tension and shear, each with its own value of η .

6 APPROXIMATE THREE-DIMENSIONAL SOLUTIONS FOR VARIOUS LOADING CASES

With the introduction of the efficiency factors η_T, η_S the reinforcement can now be analysed in a two-dimensional manner. This closely follows the work of McKenzie and Webber[2] with occasional simplifications deriving from Ref.4.

6.1 Applied radial tension

For the case of uniform radial tension σ_∞ applied at infinity the displacement v is zero and this restricts the general form of the stress function to:

$$\left.\begin{aligned} \Phi &= r_1^2\left\{\left(\frac{c_1}{1-\psi}\right)\rho^{1-\psi} + \left(\frac{c_2}{1+\psi}\right)\rho^{1+\psi}\right\} \quad , \\ &\qquad\qquad \text{in the region } r_1 < r < r_2 \quad , \\ \text{where} \qquad \psi &= \kappa^{-\frac{1}{2}} \quad , \end{aligned}\right\} \tag{6-1}$$

the c_i are arbitrary contants and the other terms have been introduced for convenience. Similarly

$$\Phi = r_1^2(c_3 \ln \rho + \tfrac{1}{2}c_4\rho^2) \quad , \qquad (6\text{-}2)$$

$$\text{in the region } r > r_2 \quad ,$$

and we note that to satisfy the conditions at infinity it is necessary that

$$c_4 = t\sigma_\infty \quad . \qquad (6\text{-}3)$$

The remaining constants are to be chosen to ensure the vanishing of $[N_r]_{r=r_1}$ and the continuity of N_r , u at $r = r_2$. Hence

$$\begin{bmatrix} 1 & 1 & 0 \\ \mu^{-\psi} & \mu^{\psi} & -\mu^{-1} \\ \mu^{-\psi}(a_{21} - \psi a_{22}) & \mu^{\psi}(a_{21} + \psi a_{22}) & \dfrac{\alpha_{22} - \alpha_{21}}{\mu t} \end{bmatrix} \begin{bmatrix} c_1 \\ c_2 \\ c_3 \end{bmatrix} = \begin{bmatrix} 0 \\ \mu t\sigma_\infty \\ (1 - \nu)\mu\sigma_\infty/E \end{bmatrix} . \qquad \ldots\ldots (6\text{-}4)$$

The stresses in the plate and reinforcement are now given by equations (4-6), (4-7) and (4-9).

6.2 Applied shear

When the applied loading at infinity is one of pure shear τ_∞ referred to cartesian coordinates at $\theta = \pm\frac{1}{4}\pi$ the stresses at infinity are such that in polar coordinates

$$\left.\begin{aligned} \sigma_r &= -\sigma_\theta = \tau_\infty \cos 2\theta \\ \tau_{r\theta} &= -\tau_\infty \sin 2\theta \quad . \end{aligned}\right\} \qquad (6\text{-}5)$$

The plate and reinforcement possess rotational symmetry about the origin and accordingly the stress function is of the form

$$\Phi = r_1^2 \cos 2\theta \sum_m C_m \rho^{q_m} \quad , \qquad (6\text{-}6)$$

where it is convenient to let $m = 1, 2, 3, 4$ refer to the region $r_1 < r < r_2$ and $m = 5, 6, 7, 8$ refer to the region $r > r_2$.

Thus from equation (4-12) we obtain the following auxiliary equation for the region $r_1 < r < r_2$,

$$\kappa(q_m - 1)^4 - (q_m - 1)^2(1 + \kappa + 8\omega) + 9 = 0 \quad , \tag{6-7}$$

whose roots are

$$\left.\begin{aligned} q_{1,2} &= 1 \pm \left[\frac{1 + \kappa + 8\omega - \left\{(1 + \kappa + 8\omega)^2 - 36\kappa\right\}^{\frac{1}{2}}}{2\kappa}\right]^{\frac{1}{2}} \quad , \\ q_{3,4} &= 1 \pm \left[\frac{1 + \kappa + 8\omega + \left\{(1 + \kappa + 8\omega)^2 - 36\kappa\right\}^{\frac{1}{2}}}{2\kappa}\right]^{\frac{1}{2}} \quad . \end{aligned}\right\} \tag{6-8}$$

Similarly in the region $r > r_2$,

$$q_{5,6,7,8} = -2, 0, 2, 4 \quad . \tag{6-9}$$

The stress resultants are given by equations (4-9) and (6-6), whence

$$\left.\begin{aligned} N_r &= \cos 2\theta \sum_m (q_m - 4)C_m\rho^{q_m - 2} \quad , \\ N_\theta &= \cos 2\theta \sum_m q_m(q_m - 1)C_m\rho^{q_m - 2} \quad , \\ N_{r\theta} &= 2 \sin 2\theta \sum_m (q_m - 1)C_m\rho^{q_m - 2} \quad , \end{aligned}\right\} \tag{6-10}$$

and we note that to satisfy the conditions at infinity, equation (6-5), it is necessary that

$$\left.\begin{aligned} C_8 &= 0 \quad , \\ C_7 &= -\tfrac{1}{2}t\tau_\infty \quad . \end{aligned}\right\} \tag{6-11}$$

It may likewise be shown that the displacements are given by

$$\left.\begin{aligned} u &= r_1 \cos 2\theta \sum_m \left\{ a_{11}\left(\frac{q_m - 4}{q_m - 1}\right) + a_{12} q_m \right\} C_m \rho^{q_m - 1} \quad , \\ v &= \tfrac{1}{2} r_1 \sin 2\theta \sum_m \left\{ a_{22} q_m (q_m - 1) - a_{11}\left(\frac{q_m - 4}{q_m - 1}\right) - 4a_{12} \right\} C_m \rho^{q_m - 1} \quad . \end{aligned}\right\} \qquad (6\text{-}12)$$

The remaining unknown coefficients C_m are now determined by the vanishing of N_r, $N_{r\theta}$ at $r = r_1$ and from the continuity of N_r, $N_{r\theta}$, u, v at $r = r_2$. These conditions yield:

$$\left.\begin{aligned} \sum_{m=1}^{4} (q_m - 4) C_m &= 0 \\ \sum_{m=1}^{4} (q_m - 1) C_m &= 0 \\ \sum_{m=1}^{4} (q_m - 4) C_m \mu^{q_m} + 6C_5 \mu^{-2} + 4C_6 &= \mu^2 t \tau_\infty \\ \sum_{m=1}^{4} (q_m - 1) C_m \mu^{q_m} + 3C_5 \mu^{-2} + C_6 &= -\tfrac{1}{2} \mu^2 t \tau_\infty \\ \sum_{m=1}^{4} \left\{ a_{11}\left(\frac{q_m - 4}{q_m - 1}\right) + a_{12} q_m \right\} C_m \mu^{q_m} - \frac{2}{Et} \left\{ (1 + \nu) C_5 \mu^{-2} + 2C_6 \right\} &= \frac{(1 + \nu)\mu^2 \tau_\infty}{E} \\ \sum_{m=1}^{4} \left\{ a_{22} q_m (q_m - 1) - a_{11}\left(\frac{q_m - 4}{q_m - 1}\right) - 4a_{12} \right\} C_m \mu^{q_m} - \frac{4}{Et} \left\{ (1 + \nu) C_5 \mu^{-2} - (1 - \nu) C_6 \right\} & \\ = \frac{-2(1 + \nu)\mu^2 \tau_\infty}{E} & \end{aligned}\right\} \qquad \ldots\ldots (6\text{-}13)$$

The stresses in the plate and reinforcement are now given by equations (6-10), (4-6) and (4-7).

6.3 Uniaxial tension

A *unit* uniaxial tensile stress applied at infinity in the direction of $\theta = 0$, say, can be split into components of uniform radial tension and pure shear in which

$$\sigma_\infty = \tau_\infty = \tfrac{1}{2} \quad . \tag{6-14}$$

The stresses in the plate and reinforcement are therefore given by appropriate addition of the stresses as determined in sections 6.1 and 6.2.

7 OPTIMUM CHOICE OF REINFORCEMENT CROSS-SECTION FOR UNIAXIAL TENSION

When the hole size, plate thickness and applied load are specified the reinforcement can be said to be optimised if, for given allowable peak stresses, the volume of reinforcement is a minimum. However, the variation of this optimum with the magnitude of the allowable peak stresses is more conveniently determined by the inverse approach in which we search for configurations which give minimum peak stresses for a given volume of reinforcement. In this connection it is convenient to introduce the following 'basic volume' V_0 defined by

$$V_0 = 2\pi r_1^2 t(E/E_\theta) \quad , \tag{7-1}$$

which enables us to express the actual volume, namely

$$V = 2\pi h(r_2^2 - r_1^2) \quad , \tag{7-2}$$

by the non-dimensional term V^* where

$$V^* = V/V_0$$

$$= \frac{(\mu^2 - 1)hE_\theta}{tE} \quad . \tag{7-3}$$

As for the weight of reinforcement we note that the density of CFRP, for example, is about 0.56 times that of aluminium and E_θ/E is typically about 2.5; accordingly a *unit* value of V^* corresponds to a *reinforcement weight which is* 0.45 *times the weight of plate removed.* It is shown later that for a

CFRP-type reinforcement on an aluminium alloy plate the practical range of values of V^* is from 0.5 to 1.0; such a method of reinforcement is therefore highly efficient.

7.1 The magnitude of the peak stresses

For the case of uniaxial tension in the direction of $\theta = 0$, the peak stresses in the reinforcement are the hoop stresses at the edge of the hole at $\theta = \pm\frac{1}{2}\pi$. The peak stresses in the plate are either the hoop stresses at the edge of the hole at $\theta = \pm\frac{1}{2}\pi$ or stresses at certain points at the junction with the reinforcing annulus at $r = r_2$. From the analysis of section 6 the peak stresses at the edge of the hole are given by equation (4-6) in which N_r, $N_{r\theta}$ are zero and

$$N_\theta = \psi(c_2 - c_1) - \sum_1^4 q_m(q_m - 1)C_m \quad , \tag{7-4}$$

and the coefficients c_1, c_2, C_m are given by equations (6-4), (6-13), (6-14). When $\nu_{\theta r} = \nu$, a condition which is effectively satisfied in all practical cases, these peak hoop stresses satisfy the relation

$$\sigma_R/E_\theta = \sigma_P/E \quad , \tag{7-5}$$

which stems from the equality of hoop strains. It is thus sufficient to confine attention to σ_P, say, which, for a unit value of the applied uniaxial stress, is numerically equivalent to a stress concentration factor. Indeed, it can also be regarded as a *strain* concentration factor, in which context it is applicable to both plate and reinforcement.

In discussing the peak stresses in the plate at $r = r_2$ it is appropriate to introduce the concept of an *equivalent* stress, and because of its convenience we adopt the Mises-Hencky version defined by

$$\sigma_{M\text{-}H} = (\sigma_r^2 - \sigma_r\sigma_\theta + \sigma_\theta^2 + 3\tau_{r\theta}^2)^{\frac{1}{2}} \quad . \tag{7-6}$$

Now from equations (6-2), (6-12), (6-13), (6-14):

$$\left.\begin{aligned} \sigma_r &= p_1 + p_2 \cos 2\theta \\ \sigma_\theta &= p_3 + p_4 \cos 2\theta \\ \tau_{r\theta} &= p_5 \sin 2\theta \quad , \end{aligned}\right\} \tag{7-7}$$

where

$$\left.\begin{aligned} p_1 &= \sigma_\infty + \frac{c_3}{t\mu^2} \\ p_2 &= \tau_\infty - \frac{6C_5}{t\mu^4} - \frac{4C_6}{t\mu^2} \\ p_3 &= \sigma_\infty - \frac{c_3}{t\mu^2} \\ p_4 &= -\tau_\infty + \frac{6C_5}{t\mu^4} \\ p_5 &= -\tau_\infty - \frac{6C_5}{t\mu^4} - \frac{2C_6}{t\mu^2} \quad . \end{aligned}\right\} \tag{7-8}$$

Thus we find

$$\sigma_{M-H} = (J_1 + J_2 \cos 2\theta + J_3 \cos^2 2\theta)^{\frac{1}{2}} \quad , \tag{7-9}$$

where

$$\left.\begin{aligned} J_1 &= p_1^2 + p_3^2 - p_1 p_3 + 3p_5^2 \\ J_2 &= 2(p_1 p_2 + p_3 p_4) - (p_2 p_3 + p_1 p_4) \\ J_3 &= p_2^2 + p_4^2 - p_2 p_4 - 3p_5^2 \quad . \end{aligned}\right\} \tag{7-10}$$

Now $\cos 2\theta$ varies between +1 at $\theta = 0, \pi$ and -1 at $\theta = \pm\frac{1}{2}\pi$, and the maximum value of σ_{M-H} therefore occurs at one of these extremes or at an intermediate point. It can be shown that the values of σ_{M-H} at these extremes, namely

$(J_1 \pm J_2 + J_3)^{\frac{1}{2}}$, are less than the peak hoop stress at $r = r_1$; accordingly σ_{M-H} is of interest only when a maximum value occurs at an intermediate value of θ , i.e. when

$$4J_3^2 > J_2^2 \quad , \tag{7-11}$$

in which case

$$\sigma_{M-H,max} = \left(J_1 - \frac{J_2^2}{4J_3}\right)^{\frac{1}{2}} \quad , \tag{7-12}$$

which occurs where

$$\theta = \tfrac{1}{2} \cos^{-1}\left(\frac{-J_2}{2J_3}\right) \quad . \tag{7-13}$$

The stress concentration factors appropriate to the hoop stress σ_P at the edge of the hole and σ_{M-H} at $r = r_2$ have been determined in the following numerical example for various values of r_1/t over a range of values of V^* , each value of V^* corresponding to a range of values of μ, h related according to equation (7-3). We consider an aluminium alloy plate with a CFRP-type reinforcement with the following elastic properties:

$$\left.\begin{aligned} E &= 70 \ \text{GPa} \\ E_\theta &= 175 \ \text{GPa} \\ E_r &= E_z = 7 \ \text{GPa} \\ G_{r\theta} &= G_{\theta z} = 2.8 \ \text{GPa} \\ G_{rz} &= 2.7 \ \text{GPa} \\ \nu &= \nu_{\theta r} = \nu_{rz} = 0.3 \quad . \end{aligned}\right\} \tag{7-14}$$

The stress concentration factors are shown in Figs.2 to 6 for values of $r_1/t = 10, 20, 30, 50, 100$ respectively; the full lines refer to σ_P and the broken lines to σ_{M-H} . However, before discussing these curves it is convenient to distinguish between those cases in which the *allowable* hoop strain in the reinforcement (ε_R , say) is greater or less than the *allowable* hoop strain in the plate (ε_P , say).

7.2 Maximum allowable hoop strains such that $\varepsilon_R \geqslant \varepsilon_P$

When the allowable hoop strain in the reinforcement exceeds that in the plate the allowable hoop stresses are such that

$$\sigma_R > \sigma_P(E_\theta/E) \quad . \tag{7-15}$$

It follows from equation (7-5) that the choice of reinforcement cross-section is dictated by the allowable stresses in the *plate*. Thus in Figs.2 to 6 we are concerned solely with the maximum stress. For example, in Fig.4 if $V^* < 0.62$ the maximum stress is always the hoop stress at $r = r_1$, but if $V^* > 0.62$ the maximum stress between typical points $\underline{a}$ and $\underline{b}$ occurs at $r = r_2$. In general, for any given value of r_1/t there is a critical value of V^* below which the maximum stress in the plate is always the hoop stress and, furthermore, there is an optimum value of r_2/r_1 which minimises the stress concentration factor; for any given value of V^* greater than the critical value there are *two* optimum values of r_2/r_1 (corresponding to points $\underline{a}$, $\underline{b}$) which 'minimise' the stress concentration factor; at these optimum values the maximum hoop stress at $r = r_1$ equals the maximum equivalent stress at $r = r_2$. The optimum values of r_2/r_1 corresponding to points $\underline{a}$ yield slightly lower stress concentration factors than those corresponding to points $\underline{b}$, but this apparent advantage is offset by the fact that the low value of reinforcement width $(r_2 - r_1)$ results in very high shear stresses in the bond between the plate and reinforcement. (This aspect is considered in greater detail in section 7.4.)

Fig.7 shows the minimum obtainable stress concentration factor for given values of r_1/t and V^* focusing attention, where necessary, on the optimum points $\underline{b}$ rather than the points $\underline{a}$. Note that Fig.7 gives a clear indication of the importance of three-dimensional shear lag effects, because if these were neglected the curves for different values of r_1/t would coincide. The reason for this marked dependence lies in the fact that with no shear lag the theoretical optimum reinforcement is a compact 'bead' which is, in practice, highly influenced by shear lag; it follows that the optimum design occurs when the deleterious effects of shear lag balance the otherwise beneficial effects of a small value of reinforcement width. The curves show that the stress concentration factor, which is 3.0 for the unreinforced hole, can be reduced to between 1.5 to 1.6 (depending upon the ratio r_1/t) by the proposed method of reinforcement. The minimum value of V^* required to achieve this reduction

varies from about 0.5 when $r_1/t = 100$ to 1.0 when $r_1/t = 10$; a further increase in the value of V^* does not cause a further reduction in the stress concentration factor.

7.3 Maximum allowable hoop strains such that $\varepsilon_R < \varepsilon_P$

When the allowable hoop strain in the reinforcement is less than that in the plate ($K\varepsilon_R = \varepsilon_P$, say) the allowable hoop stresses are such that

$$K\sigma_R = \sigma_P(E_\theta/E) \quad , \tag{7-16}$$

where $K > 1$.

It follows from equation (7-5) that the choice of reinforcement cross-section will be dictated by the hoop stresses in the reinforcement or σ_{M-H} in the plate. The stress concentration factors appropriate to σ_{M-H} are given by the broken lines in Figs.2 to 6, while *comparable* stress concentration factors for the hoop stresses in the reinforcement are given by a K-fold increase in the factors corresponding to the full lines.

Suppose, for example, that we require to optimise the reinforcement cross-section when

$$\left.\begin{aligned} r_1/t &= 30 \\ K &= 1.10 \\ V^* &= 0.8 \quad . \end{aligned}\right\} \tag{7-17}$$

The full lines in Fig.8 show the stress concentration factor in the plate derived from Fig.4 while the broken line shows the factored hoop stress concentration factors in the reinforcement, also derived from Fig.4. At points a, b the stresses in the plate and reinforcement reach their respective allowable values simultaneously. Similar curves can, of course, be drawn for different values of V^* as in section 7.1.

In general, if we compare cases in which $K > 1$ with those in which $K \leqslant 1$ it will be found that for a given value of V^* within the low range of values in which the hoop stresses are dominant, the optimum design will yield a (modified) stress concentration factor which is greater by the factor K ; alternatively the stress concentration factors can be made the same by an

increase in V^* . For given values of V^* in the higher range of values in which the hoop stresses and σ_{M-H} are of equal importance, the stress concentration factors are still greater, but by factors which vary between K and some number only slightly greater than unity.

7.4 Bond strength and off-optimum designs

We have already mentioned that low values of the reinforcement width can cause unacceptably high shear stresses in the bond between the plate and reinforcement. A measure of the peak load/unit length in the plate at $r = r_2$ is given by $t\sigma_{M-H}$ and the *average* shear stress in the bond is therefore given approximately by

$$\tau_{bond,av} \approx \frac{t\sigma_{M-H}}{2(r_2 - r_1)} \quad . \tag{7-18}$$

The peak shear stress will be greater than this because of variations across the width and it would be prudent to assume that

$$\tau_{bond,max} = 2\tau_{bond,av} \quad , \quad \text{say} \quad . \tag{7-19}$$

Indeed, very high but localised shear stresses occur near $r = r_2$ because of the 90 degree re-entrant angle[1]. However, these can be avoided by tapering the outer edges of the discs so that the re-entrant angle is increased to 135 degrees, say; of course, in the analysis r_2 will then refer to an average value.

Consider now the following example: if $r_1/t = 30$ we see from Fig.7 that the stress concentration factor can be reduced to 1.55 by taking $V^* = 0.6$. Fig.4 shows that this is possible if

$$r_2/r_1 = 1.082 \quad ,$$

whence, from equations (7-3), (7-14)

and

$$\left.\begin{aligned} r_2 - r_1 &= 2.46t \\ h &= 1.40t \quad . \end{aligned}\right\} \tag{7-20}$$

Similarly from equations (7-19), (7-20)

$$\tau_{bond,max} = 0.406\sigma_{M-H} \quad . \tag{7-21}$$

Now if the allowable stresses are such that

$$\tau_{bond} = 60 \text{ MPa}$$

$$\sigma_{M-H} = 200 \text{ MPa} \quad , \quad \text{say} \quad ,$$

it follows that $\tau_{bond,max}$ must not exceed $0.3\sigma_{M-H}$. The theoretical optimum design specified by equation (7-20) will therefore fail prematurely in the bond. However, this problem can be overcome without an increase in the weight of reinforcement and with negligible increase in the stress concentration factor by the adoption of an off-optimum design in which

$$r_2 - r_1 = 3.33t$$

so that

$$r_2/r_1 = 1.111 \quad ,$$

which results in a stress concentration factor only about 1% greater than the theoretical minimum.

The above example highlights the fact that for a given weight of reinforcement it may be advantageous to choose an off-optimum design in which r_2/r_1 is greater than that required to minimise the stress concentration factor. This is because the slight increase in stress concentration factor will be offset by a marked reduction in the shear stresses in the bond and a marked reduction in the thickness h .

8 CONCLUSIONS

A simplified technique is presented for the stress analysis and optimum design of fibre reinforced annular discs surrounding a circular hole in a flat plate under various loading conditions. The method allows for shear lag effects normal to the plane of the plate. For the practically important case of applied uniaxial stress it is shown that the optimum design of reinforcement is markedly dependent on these shear lag effects. Detailed numerical results are given for an aluminium alloy plate with a CFRP reinforcement. The lightest

reinforcement which reduces the hoop stress concentration factor to a prescribed amount is shown to depend on the ratio (hole diameter)/(plate thickness). Typically, a stress concentration factor between 1.5 and 1.6 can be achieved with a reinforcement whose weight is between 0.3 and 0.6 times that of the plate removed.

Acknowledgment

The author is much indebted to Doreen Bartholomew for the computation.

REFERENCES

No.	Author	Title, etc.
1	E.H. Mansfield	Three-dimensional stress analysis of cylindrically wound fibre reinforced annular discs surrounding a circular hole in a flat plate. Int. J. Mech. Sci., Vol.18, pp 469-479 (1976)
2	D.O. McKenzie J.P.H. Webber	Hole reinforcement in isotropic and orthotropic plates using filament-wound discs. Aero. Quart. Vol.XXVI, Part 4, pp.254-74 (1975)
3	S.G. Lekhnitskii	*Anisotropic plates.* Translated from the second Russian edition by S.W. Tsai and T. Cheron. Gordon and Breach (1968)
4	E.H. Mansfield	Stress analysis of fibre reinforced plates with polar orthotropy. ARC R & M 3796 (1975)
5	S.P. Timoshenko S. Woinowsky-Krieger	*Theory of plates and shells.* Second Edition. McGraw-Hill Book Co. (1959)

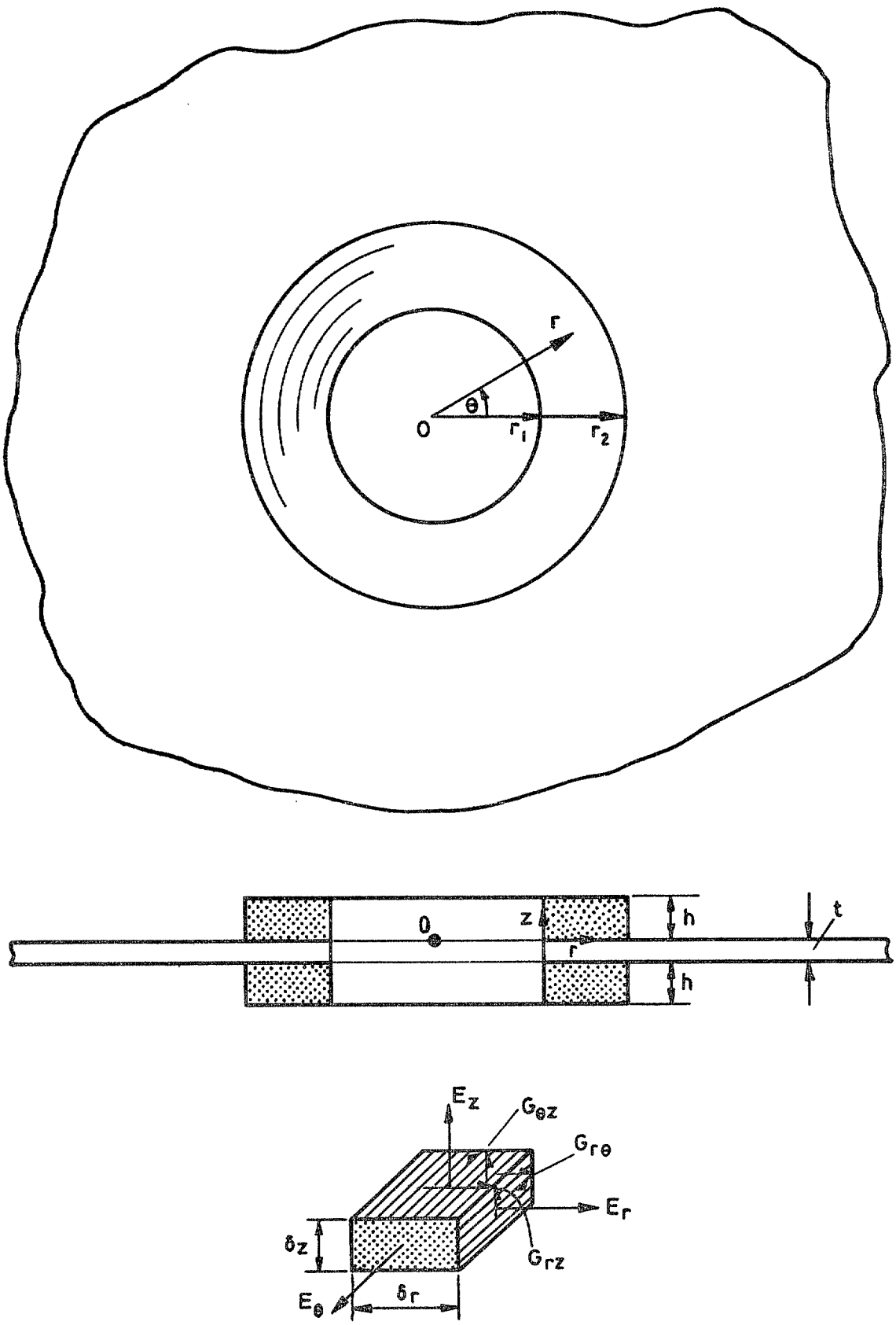

Fig.1 The plate and annular reinforcement

Fig.2

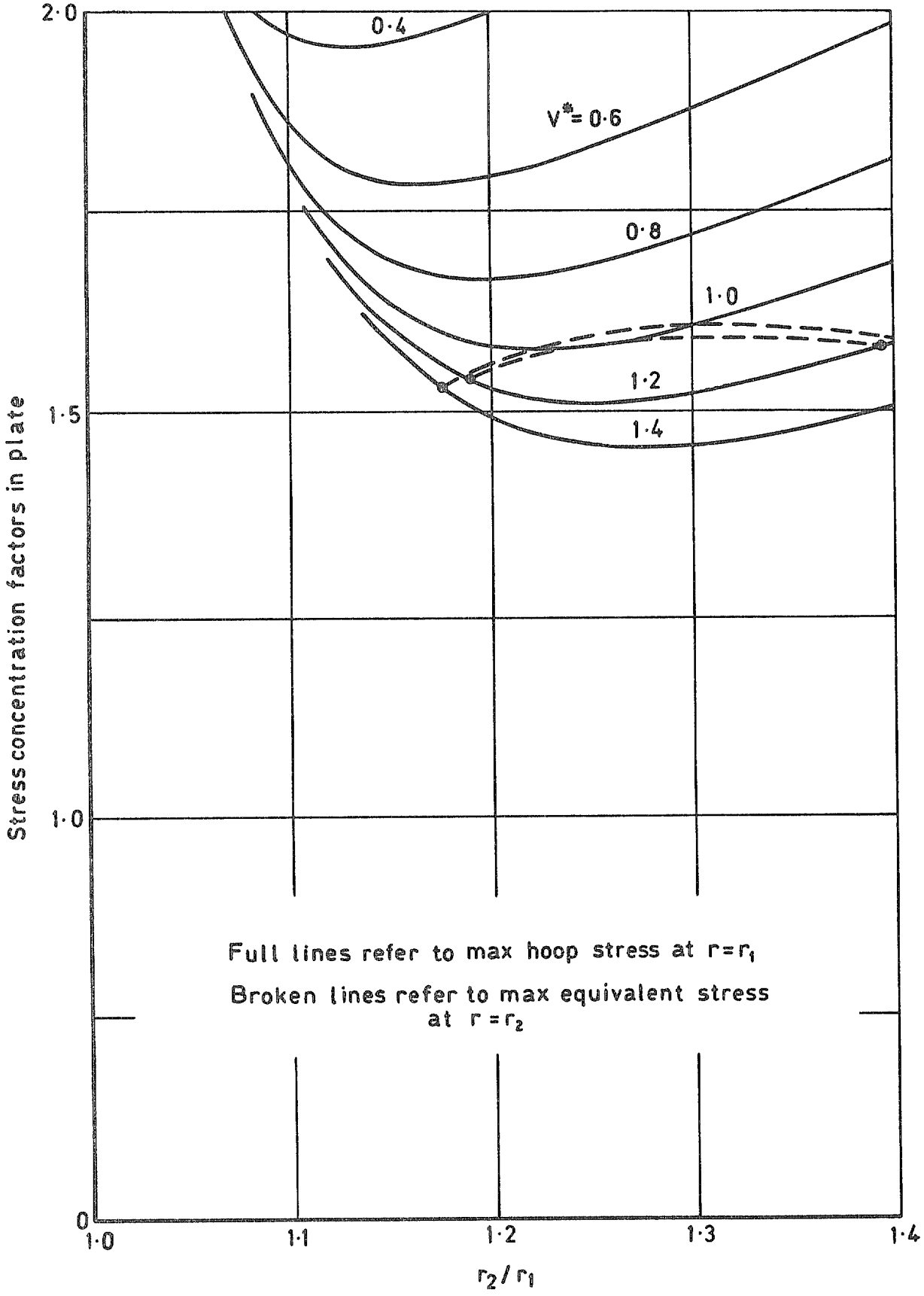

Fig.2 Variation of stress concentration factors with V^*, r_2/r_1 for $r_1/t = 10$

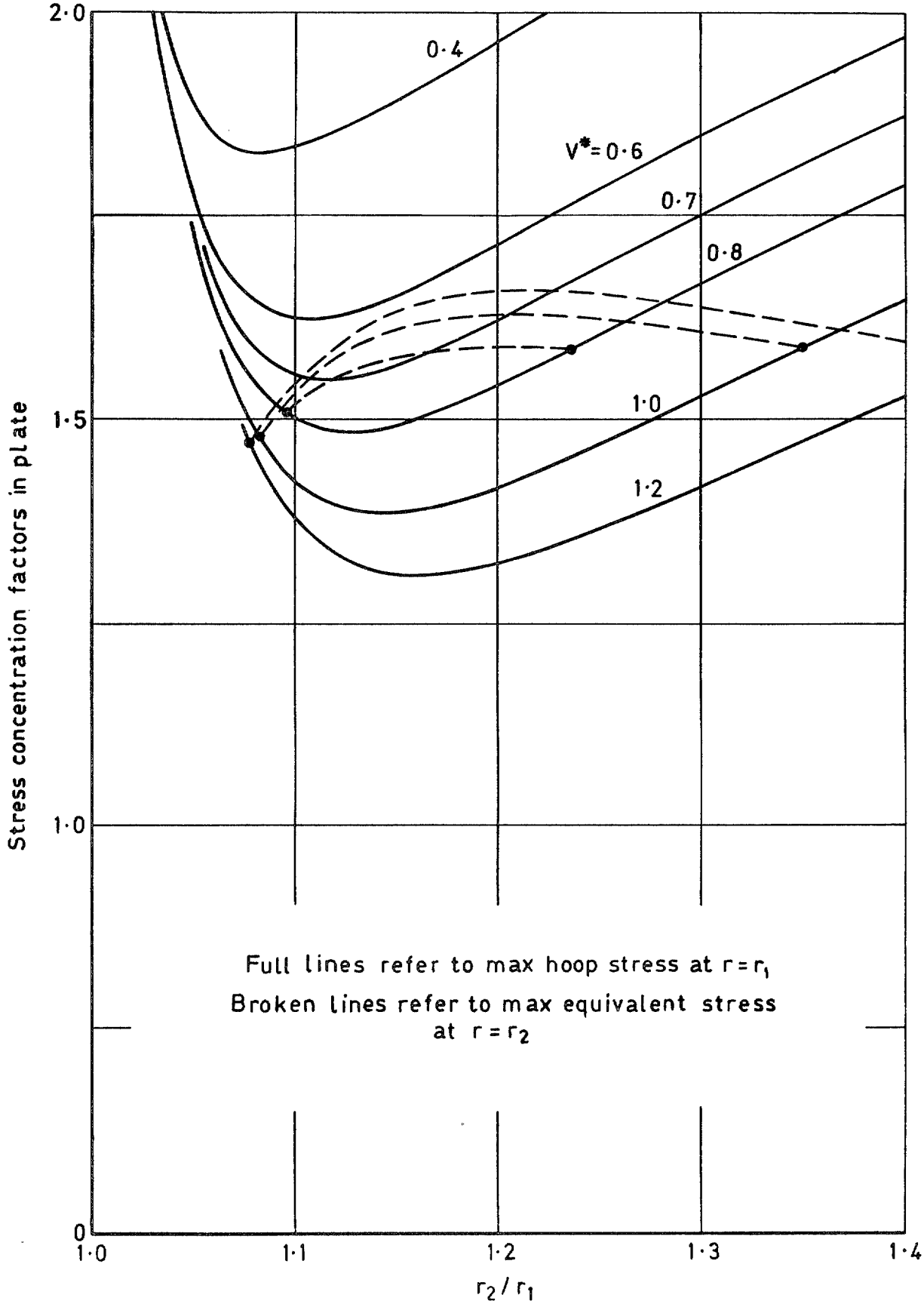

Fig.3 Variation of stress concentration factors with V^*, r_2/r_1 for $r_1/t = 20$

Fig.4

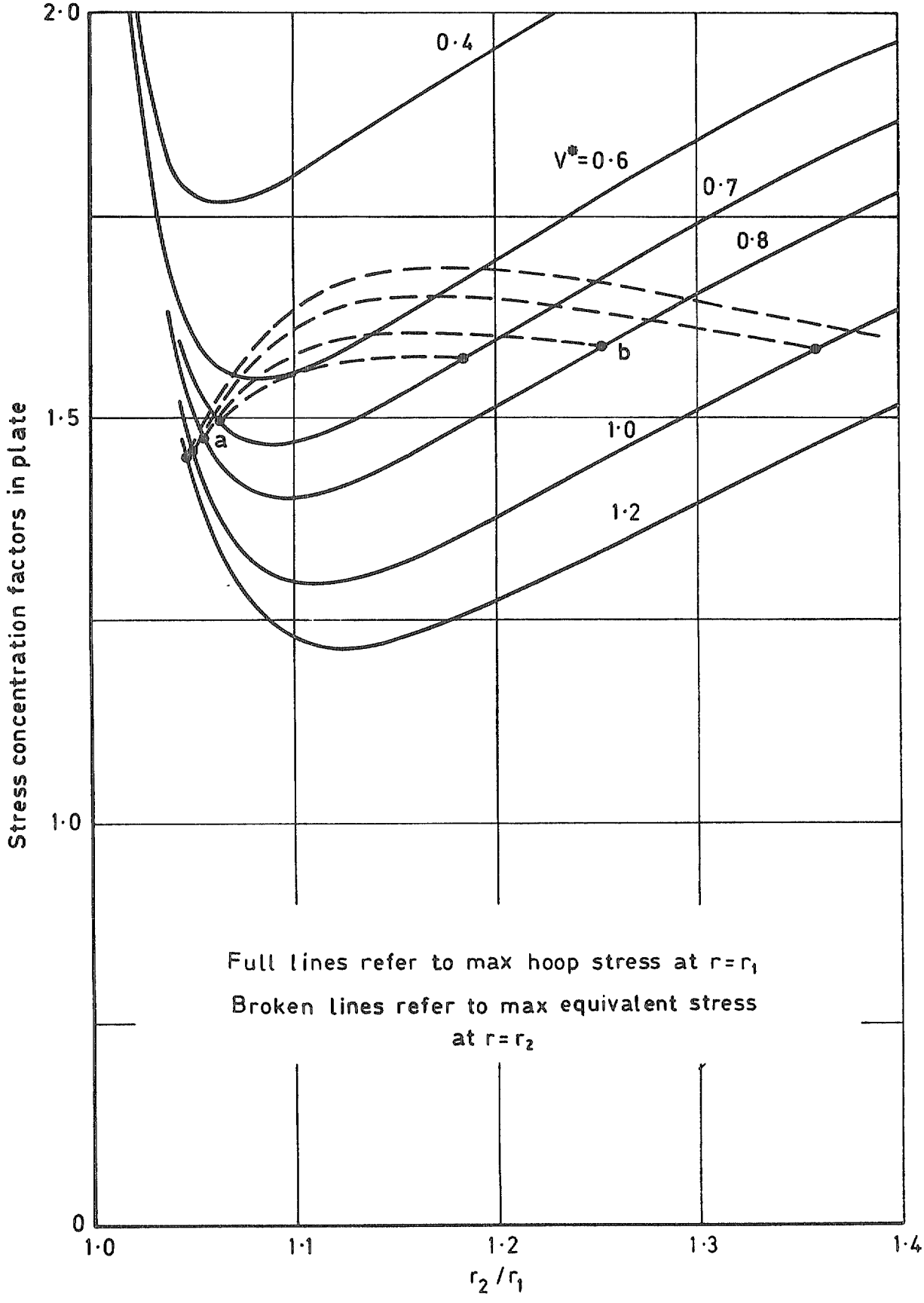

Fig.4 Variation of stress concentration factors with $V^*, r_2/r_1$ for $r_1/t = 30$

Fig.5

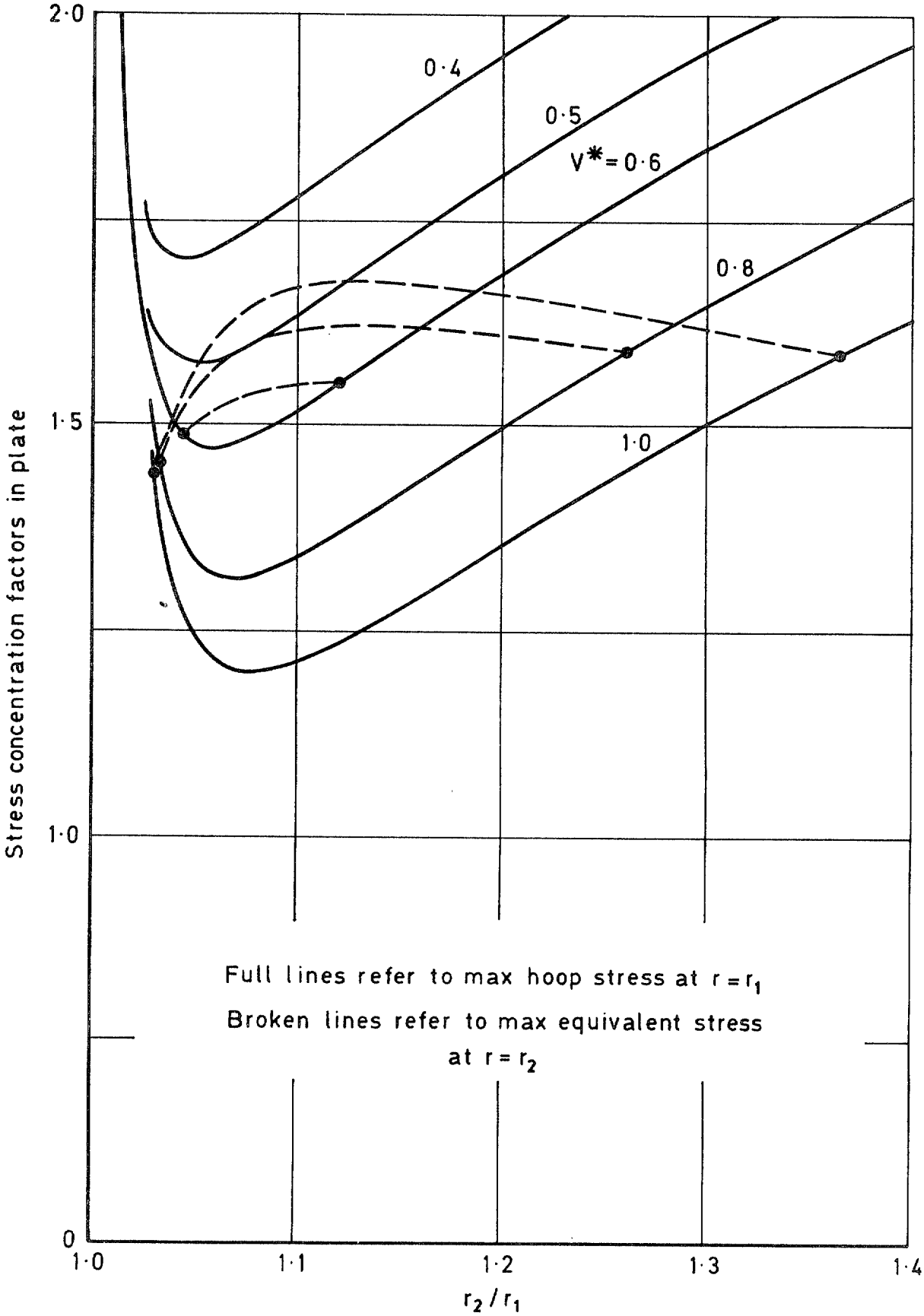

Fig.5 Variation of stress concentration factors with V^*, r_2/r_1 for $r_1/t = 50$

Fig.6

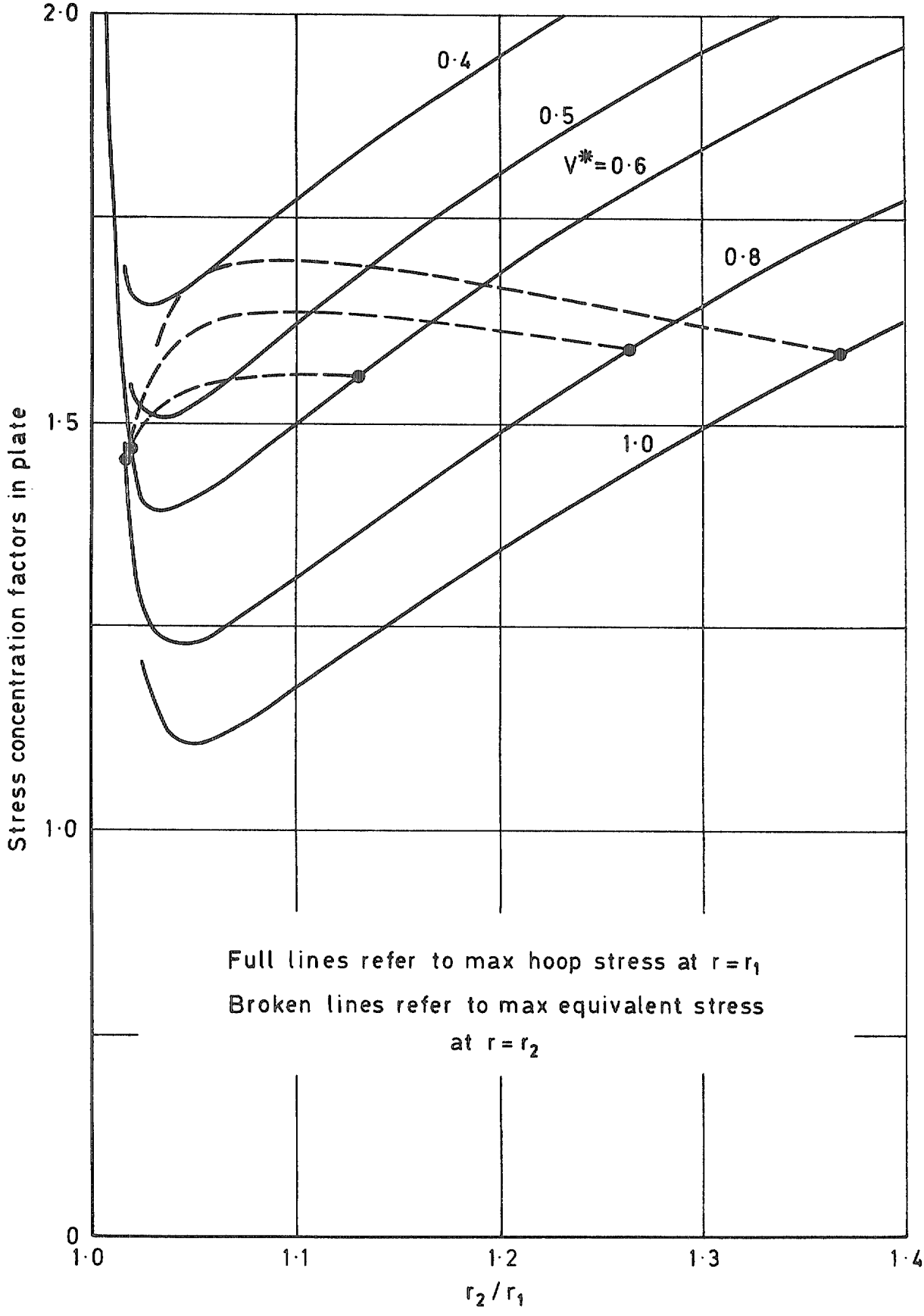

Fig.6 Variation of stress concentration factors with V^*, r_2/r_1 for $r_1/t=100$

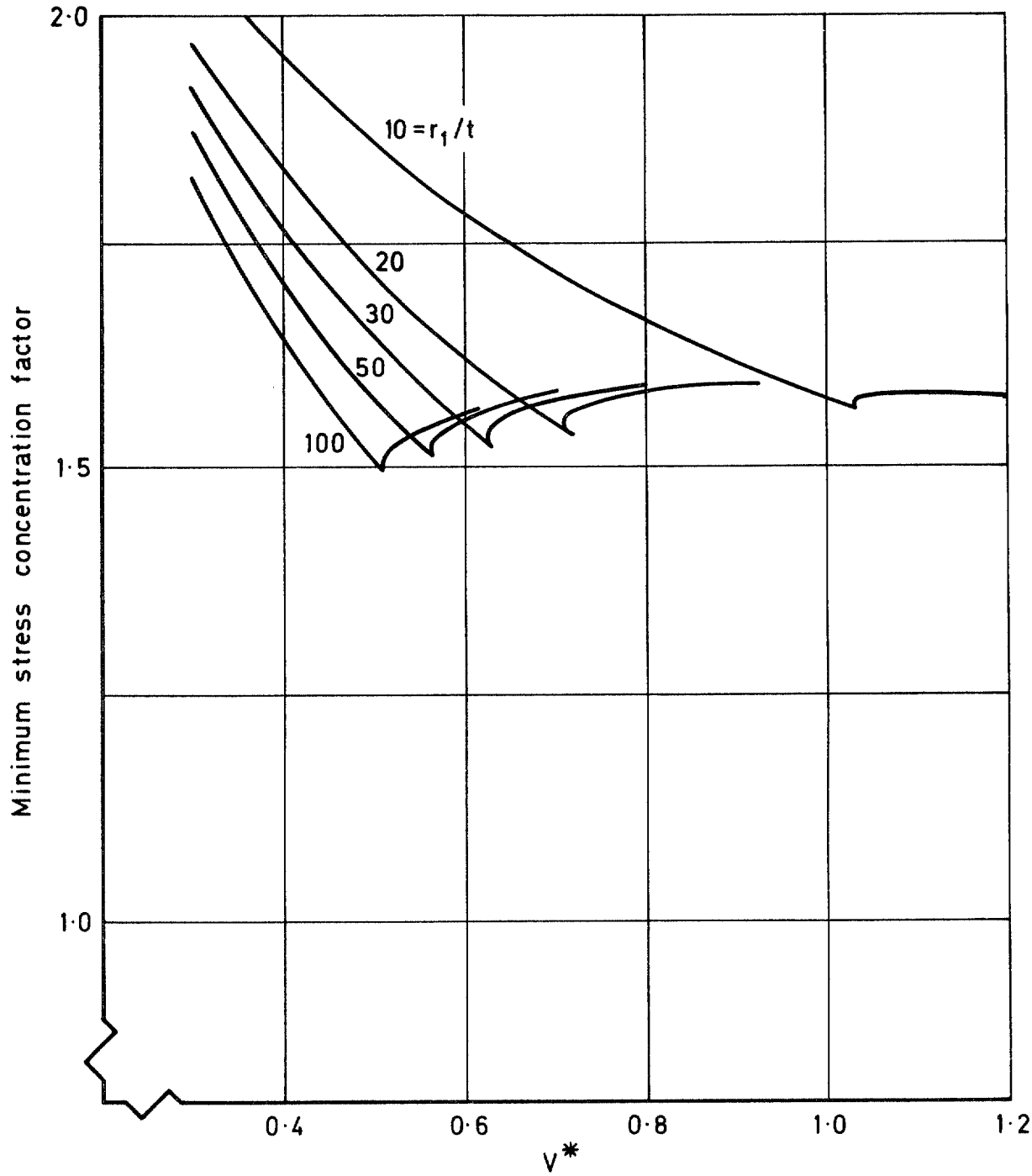

Fig. 7 Variation of minimum obtainable stress concentration factor with V^*

Fig.8

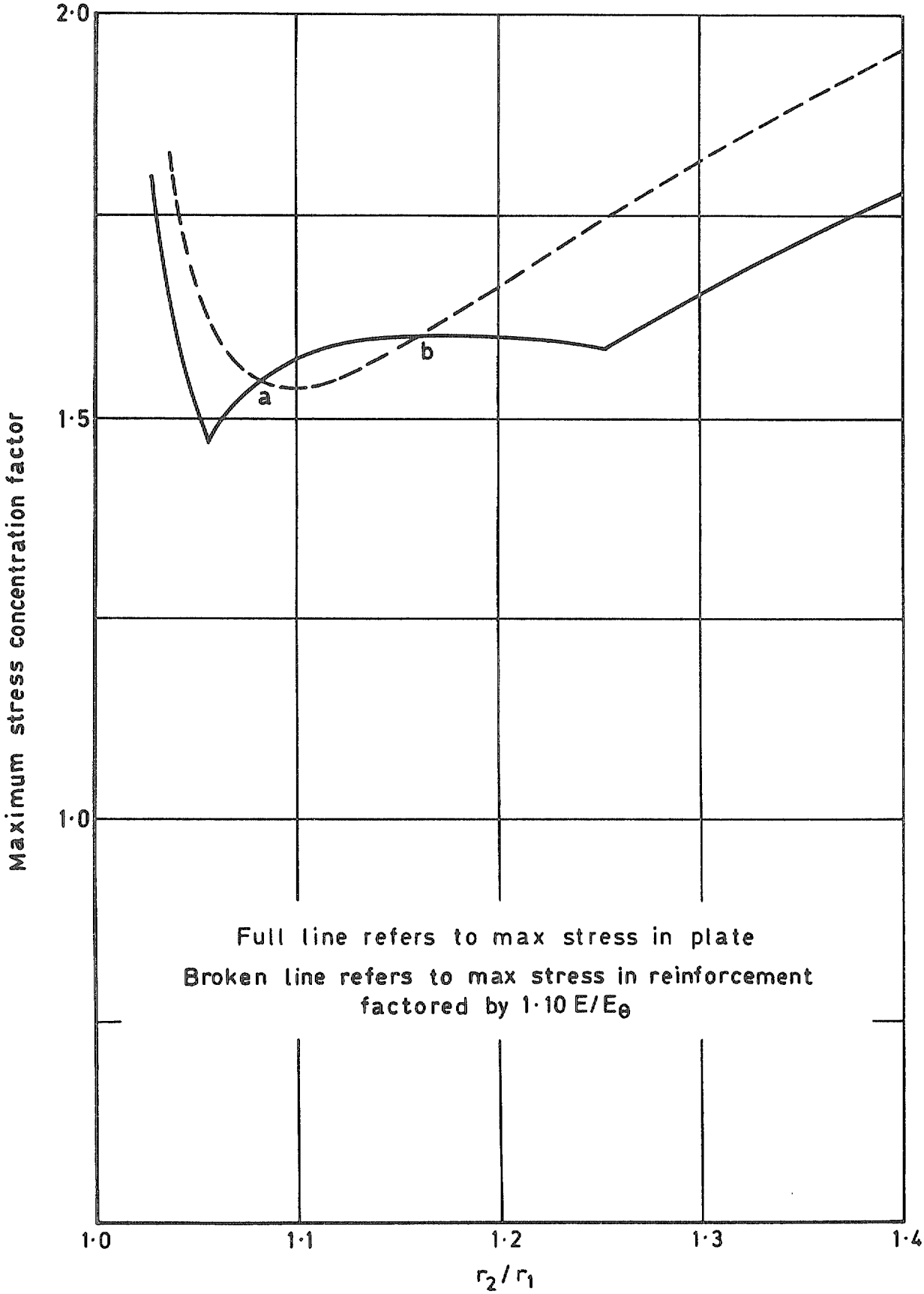

Fig.8 Variation of stress concentration factors with r_2/r_1, $r_1/t = 30$, $V^* = 0{\cdot}8$

Printed in England for Her Majesty's Stationery Office by the Royal Aircraft Establishment, Farnborough. Dd. 587484 K5 1/78.

1978

Published by
HER MAJESTY'S STATIONERY OFFICE

Government Bookshops
49 High Holborn, London WC1V 6HB
13a Castle Street, Edinburgh EH2 3AR
41 The Hayes, Cardiff CF1 1JW
Brazennose Street, Manchester M60 8AS
Southey House, Wine Street, Bristol BS1 2BQ
258 Broad Street, Birmingham B1 2HE
80 Chichester Street, Belfast BT1 4JY

Government Publications are also available through booksellers

R &M No.3815
ISBN 0 11 471148 8